IMMUNOLOGY

Novel CD11b$^+$Gr-1$^+$Sca-1$^+$ myeloid cells drive mortality in bacterial infection

Min Young Park[1]*, Hyung Sik Kim[1]*, Ha Young Lee[1], Brian A. Zabel[2], Yoe-Sik Bae[1,3†]

Extreme pathophysiological stressors induce expansion of otherwise infrequent leukocyte populations. Here, we found a previously unidentified CD11b$^+$Gr-1$^+$ myeloid cell population that expresses stem cell antigen-1 (Sca-1) induced upon experimental infection with *Staphylococcus aureus*. Although CD11b$^+$Gr-1$^+$Sca-1$^+$ cells have impaired migratory capacity and superoxide anion–producing activity, they secrete increased levels of several cytokines and chemokines compared to Sca-1$^-$ counterparts. The generation of CD11b$^+$Gr-1$^+$Sca-1$^+$ cells is dependent on IFN-γ in vivo, and in vitro stimulation of bone marrow cells or granulocyte-macrophage progenitors with IFN-γ generated CD11b$^+$Gr-1$^+$Sca-1$^+$ cells. Depletion of CD11b$^+$Gr-1$^+$Sca-1$^+$ cells by administrating anti–Sca-1 antibody strongly increased survival rates in an *S. aureus* infection model by reducing organ damage and inflammatory cytokines. However, adoptive transfer of CD11b$^+$Gr-1$^+$Sca-1$^+$ cells decreased survival rates by worsening the pathogenesis of *S. aureus* infection. Together, we found a previously unidentified pathogenic CD11b$^+$Gr-1$^+$Sca-1$^+$ population that plays an essential role in mortality during bacterial infection.

INTRODUCTION

CD11b$^+$ myeloid cells play essential roles in innate immune responses through the phagocytosis and killing of invading pathogenic microorganisms (*1*). Neutrophils, a subset of mature differentiated CD11b$^+$ myeloid cells, are the first leukocytes recruited to sites of infection, where they play an essential role in host defense via phagocytosis and myeloperoxidase (MPO)–dependent pathogen killing (*2*, *3*). Monocytes, another subset of mature CD11b$^+$ myeloid cells, migrate to an infected area, differentiate into macrophages, and contribute to host defense by phagocytosis, antigen presentation, and cytokine release (*4*, *5*). A heterogeneous population of immature bone marrow myeloid cells expressing CD11b and Gr-1 (including two isoforms of Ly6C and Ly6G) gives rise to different types of mature CD11b$^+$ myeloid cells (*6*).

Others have reported that phenotypically and morphologically heterogeneous CD11b$^+$Gr-1$^+$ myeloid cells are expanded in tissues of bacteria-infected mice or tumor-bearing mice (*7*, *8*). The most well-characterized pathophysiologically induced population of CD11b$^+$Gr-1$^+$ myeloid cells are myeloid-derived suppressor cells (MDSCs) (*9*). MDSCs, which express CD11b$^+$Gr-1$^+$ as minimal phenotypical characteristics but are in many other ways heterogeneous, are implicated in the suppression of immune cells (especially T lymphocytes) via production of arginases, nitric oxide, reactive oxygen species, indoleamine 2, 3-dioxygenase (IDO), and transforming growth factor–β (TGF-β) (*9*–*11*). One of the major functional roles of MDSCs is suppressing antitumor immunity, tumor angiogenesis, and tumor metastasis (*8*, *12*, *13*). MDSCs also suppress inflammation and promote insulin sensitivity in obesity (*14*). Given the abundance and heterogeneity of CD11b$^+$Gr-1$^+$ myeloid cells as MDSCs, we hypothesized that additional unidentified CD11b$^+$Gr-1$^+$ myeloid cell populations are induced by other pathological conditions characterized by immune dysregulation and similarly play essential roles in disease pathogenesis.

Stem cell antigen-1 (Sca-1), a mouse glycosyl phosphatidylinositol-anchored protein, is a marker for mouse hematopoietic stem cells (HSCs) (*15*). Recent evidence demonstrated that Sca-1 expression is in fact not limited to HSCs but is also expressed in several differentiated mature leukocyte types such as dendritic cells, B lymphocytes, and monocytes, and is induced on bone marrow cells following bacterial infection (*16*–*18*). Given the critical role of CD11b$^+$ myeloid cells in both protections against invading microorganisms and in pathogenic host responses to systemic bacterial infection (e.g., septicemia), we sought to further identify and characterize bacterial infection–induced CD11b$^+$Gr-1$^+$ myeloid cell populations by focusing on Sca-1 expression.

RESULTS

A previously unidentified CD11b$^+$Gr-1$^+$Sca-1$^+$ myeloid cell population is generated upon experimental *Staphylococcus aureus* (*S. aureus*) infection

We examined whether experimental infection with *S. aureus*, a Gram-positive bacterium that is a major contributor to sepsis in human patients, induces different CD11b$^+$Gr-1$^+$ myeloid cell populations in mice. Wild-type (WT) mice were intraperitoneally injected with *S. aureus* [1×10^7 colony-forming units (CFUs) per head]. *S. aureus* infection caused increases in both CD11b$^+$Gr-1$^+$Sca-1$^-$ and CD11b$^+$Gr-1$^+$Sca-1$^+$ myeloid cell populations in peritoneal fluid exudates collected 24 hours after inoculation (Fig. 1A). CD11b$^+$Gr-1$^+$Sca-1$^+$ myeloid cell populations showed slightly increased size but similar granularity compared to CD11b$^+$Gr-1$^+$Sca-1$^-$ myeloid cells (Fig. 1B, top). The expression of monocyte-associated markers such as Ly6C, CCR2, and CX3CR1 (but not CD115) is slightly higher in CD11b$^+$Gr-1$^+$Sca-1$^+$ than in CD11b$^+$Gr-1$^+$Sca-1$^-$ myeloid cell populations (Fig. 1B, middle and bottom). A previous study noted that mature neutrophils are Ly6G$^+$CXCR2$^+$CD101$^+$, whereas immature neutrophils are Ly6G$^{lo/+}$CXCR2$^-$CD101$^-$ (*19*). Here, we found that the expression of these neutrophil-associated markers (Ly6G, CXCR2, and CD101) was apparent in CD11b$^+$Gr-1$^+$Sca-1$^-$ but not in CD11b$^+$

[1]Department of Biological Sciences, Sungkyunkwan University, Suwon 16419, Republic of Korea. [2]Palo Alto Veterans Institute for Research, Veterans Affairs Hospital, Palo Alto, CA 94304, USA. [3]Department of Health Sciences and Technology, SAIHST, Sungkyunkwan University, Seoul 06351, Republic of Korea.
*These authors contributed equally to this work.
†Corresponding author. Email: yoesik@skku.edu

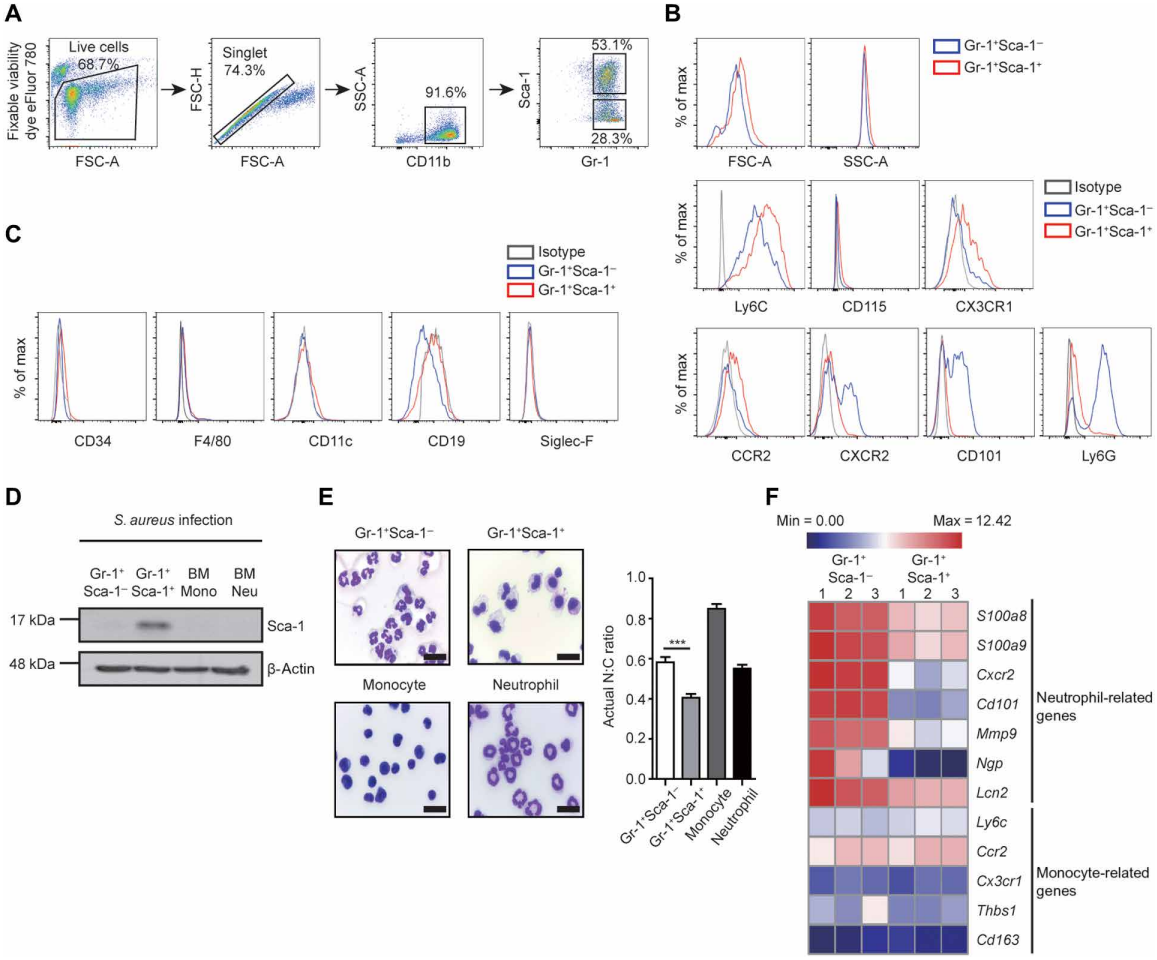

Fig. 1. Expansion of CD11b$^+$Gr-1$^+$Sca-1$^+$ myeloid cells in *S. aureus*–infected mice. (**A** to **C**) WT mice were infected with *S. aureus* (1×10^7 CFUs per head, intraperitoneal injection). Peritoneal fluid was collected 24 hours after infection. (A) Flow cytometry gating strategy: CD11b$^+$ peritoneal cells were stained with anti–Sca-1 and anti–Gr-1 antibody. CD11b$^+$Gr-1$^+$Sca-1$^-$ and CD11b$^+$Gr-1$^+$Sca-1$^+$ myeloid cells were analyzed with markers of monocytes (Ly6C, CD115, CX3CR1, and CCR2), neutrophils (CXCR2, CD101, and Ly6G) (B), and other cell types (C) by flow cytometry. (**D** and **E**) CD11b$^+$Gr-1$^+$Sca-1$^-$, CD11b$^+$Gr-1$^+$Sca-1$^+$ cells, bone marrow monocytes (BM Mono), and bone marrow neutrophils (BM Neu) were sorted from *S. aureus* (1×10^7 CFUs per head)–infected mice. The cells were analyzed by Western blot for Sca-1 and β-actin protein expression (D) or stained by Giemsa staining solution with quantification of the actual N:C ratio (nuclear-to-cytoplasmic ratio). Scale bars, 20 μm (E). (**F**) Transcriptional analysis of sorted CD11b$^+$Gr-1$^+$Sca-1$^-$ and CD11b$^+$Gr-1$^+$Sca-1$^+$ myeloid cells. The data are representative of three independent experiments (B to E, left). Data are expressed as means ± SEM ($n = 8$ for E, right). ***$P < 0.001$ by Student's *t* test. FSC-A, forward scatter area; FSC-H, forward scatter height; SSC-A, side scatter area.

Gr-1$^+$Sca-1$^+$ myeloid cell populations (Fig. 1B, bottom). Flow cytometry analysis also revealed that both CD11b$^+$Gr-1$^+$Sca-1$^-$ and CD11b$^+$Gr-1$^+$Sca-1$^+$ myeloid cell populations were negative for CD34, F4/80, CD11c, CD19, and Siglec-F (Fig. 1C), indicating that they are not HSCs, macrophages, dendritic cells, B lymphocytes, or eosinophils. Because CD11b$^+$Gr-1$^+$Sca-1$^-$ and CD11b$^+$Gr-1$^+$Sca-1$^+$ cell populations are of myeloid origin, we further compared the two populations with bone marrow monocytes and bone marrow neutrophils. Sca-1 expression was limited to only the *S. aureus* infection–induced peritoneal CD11b$^+$Gr-1$^+$Sca-1$^+$ myeloid cells (Fig. 1D). By Giemsa staining, sorted CD11b$^+$Gr-1$^+$Sca-1$^+$ myeloid cells had a banded morphology consistent with immature myeloid cells, while the sorted CD11b$^+$Gr-1$^+$Sca-1$^-$ myeloid cells had a segmented morphology consistent with mature neutrophils (Fig. 1E, left). CD11b$^+$Gr-1$^+$Sca-1$^+$ myeloid cells also had significantly lower nucleus-to-cytoplasm ratios than CD11b$^+$Gr-1$^+$Sca-1$^-$, consistent with respective immature myeloid and mature neutrophil phenotypes cells (Fig. 1E, right). Sorted CD11b$^+$Gr-1$^+$Sca-1$^+$ myeloid cells expressed markedly lower levels of neutrophil-related genes (*S100a8*, *S100a9*, *Cxcr2*, *Cd101*, *Mmp9*, *Ngp*, and *Lcn2*) than CD11b$^+$Gr-1$^+$Sca-1$^-$ cells by transcriptome analysis (Fig. 1F and data file S1). Both populations expressed low levels of monocyte-related genes (*Ly6c*, *Ccr2*, *Cx3cr1*, *Thbs1*, and *Cd163*) (Fig. 1F and data file S1).

S. aureus infection induced systemic expansion of CD11b$^+$Gr-1$^+$Sca-1$^+$ myeloid cells, as increased percentages were detected in the bone marrow, peritoneal fluid, peripheral blood, and spleen compared to uninfected controls (fig. S1A). CD11b$^+$Gr-1$^+$Sca-1$^+$ myeloid cells were significantly expanded by 12 hours after infection and continued to increase until 24 hours after infection (fig. S1B). The generation of CD11b$^+$Gr-1$^+$Sca-1$^+$ myeloid cells was not limited to in vivo exposure to only live Gram-positive *S. aureus*, as experimental exposure to heat-killed Gram-positive *S. aureus*, Gram-negative *Escherichia coli* (*E. coli*), zymosan, or lipoteichoic acid (LTA; Gram-positive bacteria cell wall component) also induced CD11b$^+$Gr-1$^+$Sca-1$^+$ myeloid cells in the peritoneal fluid, although not to the extent observed with *S. aureus* (fig. S1C).

CD11b$^+$Gr-1$^+$Sca-1$^+$ myeloid cells have impaired migratory activity, superoxide anion production, but produce abundant amounts of inflammatory cytokines

Since leukocyte trafficking is critical to both the protective (localization to invading microorganisms to enable effective killing) and pathological (vital organ infiltration and collateral tissue damage) features of the immune response to pathogens, we next assessed chemoattractant receptor expression and function in CD11b$^+$Gr-1$^+$Sca-1$^-$ and CD11b$^+$Gr-1$^+$Sca-1$^+$ myeloid cell populations. By RNA expression analysis, the levels of *Fpr1/2*, *Cxcr1/2*, and *C5ar* were significantly reduced in CD11b$^+$Gr-1$^+$Sca-1$^+$ myeloid cells compared to CD11b$^+$Gr-1$^+$Sca-1$^-$ myeloid cells (Fig. 2A). We then examined the functional migratory responses of CD11b$^+$Gr-1$^+$Sca-1$^-$ and CD11b$^+$Gr-1$^+$Sca-1$^+$ myeloid cells to several chemoattractants. While CD11b$^+$Gr-1$^+$Sca-1$^-$ myeloid cells migrated substantially to fMLF (FPR1 ligand), WKYMVm (FPR1/2 ligand), C5a (C5aR ligand), and CXCL2 (CXCR1/2 ligand), CD11b$^+$Gr-1$^+$Sca-1$^+$ myeloid cells did not markedly migrate to these chemoattractants (Fig. 2B).

Certain CD11b$^+$ myeloid cells remove invading pathogens via phagocytic activity and subsequent bacteria killing (*20*). In this study, we compared the phagocytic activity of CD11b$^+$Gr-1$^+$Sca-1$^-$ and CD11b$^+$Gr-1$^+$Sca-1$^+$ myeloid cells using live *E. coli*, *S. aureus*, or latex beads that were labeled with fluorescent dyes. Engulfment of *E. coli*, *S. aureus*, or latex beads was similar for CD11b$^+$Gr-1$^+$Sca-1$^-$ and CD11b$^+$Gr-1$^+$Sca-1$^+$ myeloid cells (fig. S2). These results suggest that bacteria-directed phagocytosis is similar in CD11b$^+$Gr-1$^+$Sca-1$^-$ and CD11b$^+$Gr-1$^+$Sca-1$^+$ myeloid cells. Reactive oxygen species such as superoxide anion are important weapons used by certain myeloid cells such as neutrophils to kill invading pathogens (*21*). In this study, we measured superoxide anion production by CD11b$^+$Gr-1$^+$Sca-1$^-$ and CD11b$^+$Gr-1$^+$Sca-1$^+$ myeloid cells following stimulation with phorbol 12-myristate 13-acetate (PMA), well known to

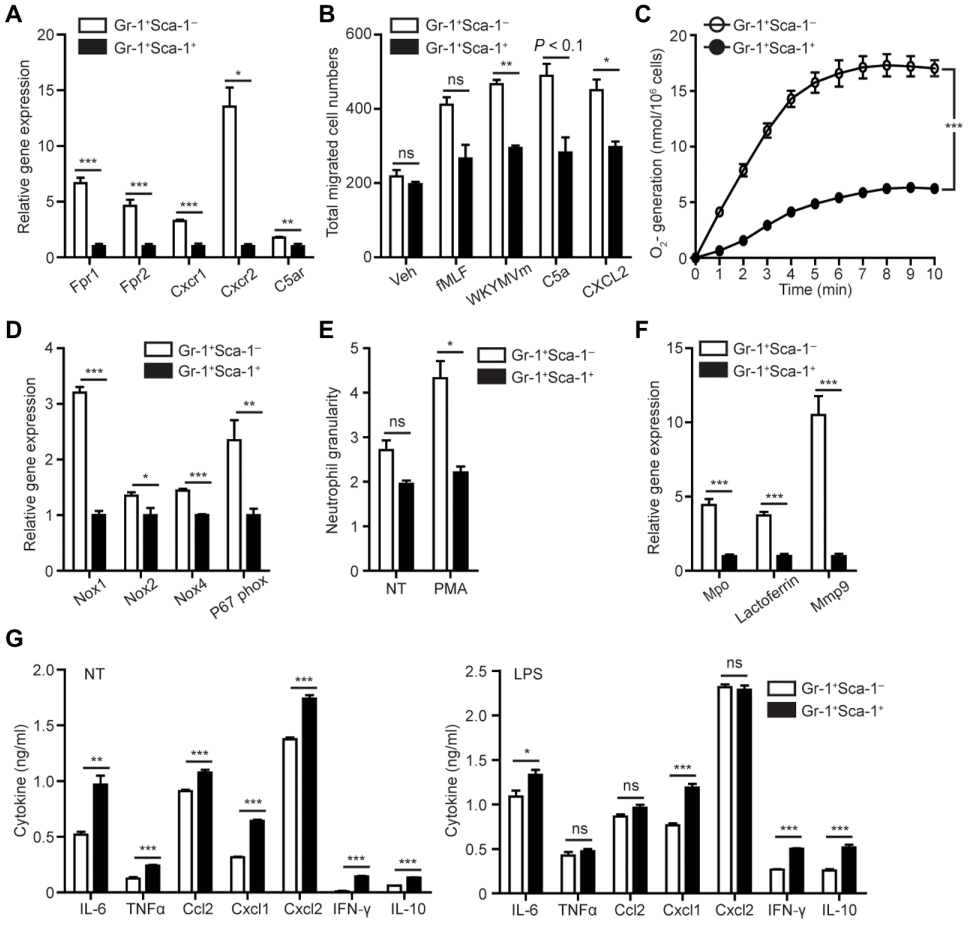

Fig. 2. Comparison of chemotactic activity, innate immunity, and cytokine production between CD11b$^+$Gr-1$^+$Sca-1$^-$ and CD11b$^+$Gr-1$^+$Sca-1$^+$ myeloid cells. (**A** to **G**) WT mice were infected with *S. aureus* (1×10^7 CFUs per head, intraperitoneal injection). Peritoneal fluids were collected 24 hours after infection, and CD11b$^+$Gr-1$^+$Sca-1$^-$ and CD11b$^+$Gr-1$^+$Sca-1$^+$ myeloid cells were sorted and analyzed. (A) The expression of chemoattractant receptors was analyzed by reverse transcription quantitative polymerase chain reaction (RT-qPCR). (B) Chemotaxis to vehicle control (negative control/basal migration), fMLF (1 μM), WKYMVm (1 μM), C5a (10 ng/ml), and CXCL2 (30 ng/ml) was measured 90 min after cell loading. (C) Superoxide production was measured from isolated CD11b$^+$Gr-1$^+$Sca-1$^-$ and CD11b$^+$Gr-1$^+$Sca-1$^+$ populations after stimulation with PMA (1 μM) by the cytochrome c reduction assay. (D) The expression of superoxide anion production–related genes was analyzed by RT-qPCR. (E) Degranulation was measured after stimulation with PMA (1 μM) by the β-hexosaminidase assay. (F) The expression of granule component was analyzed by RT-qPCR. (G) Sorted CD11b$^+$Gr-1$^+$Sca-1$^-$ and CD11b$^+$Gr-1$^+$Sca-1$^+$ myeloid cells were stimulated with LPS (1 μg/ml) or incubated without stimulation (NT, no treatment) for 24 hours. The levels of cytokines and chemokines were measured by enzyme-linked immunosorbent assay (ELISA) from collected supernatants. Data are expressed as means ± SEM ($n = 6$ for A, B, and D to G, and $n = 3$ for C). *$P < 0.05$, **$P < 0.01$, and ***$P < 0.001$ by Student's *t* test (A, B, and D to G) or using two-way analysis of variance (ANOVA) (C). ns, not significant.

induce superoxide anion. PMA strongly stimulated superoxide anion production from CD11b$^+$Gr-1$^+$Sca-1$^-$ myeloid cells but not from CD11b$^+$Gr-1$^+$Sca-1$^+$ myeloid cells (Fig. 2C). We then analyzed the expression profile of genes critical to effective superoxide anion production. CD11b$^+$Gr-1$^+$Sca-1$^+$ myeloid cells expressed significantly lower levels of NADPH (reduced form of nicotinamide adenine dinucleotide phosphate) oxidase complex components (encoded by *Nox1*, *Nox2*, *Nox4*, and *P67 phox*) compared to CD11b$^+$Gr-1$^+$Sca-1$^-$ myeloid cells (Fig. 2D). Certain myeloid cells release granule contents upon stimulation (*22*). We next compared degranulation activity in the two CD11b$^+$Gr-1$^+$ myeloid cell populations. PMA stimulation induced substantially more degranulation by CD11b$^+$Gr-1$^+$Sca-1$^-$ cells than CD11b$^+$Gr-1$^+$Sca-1$^+$ cells (Fig. 2E). RNA expression analysis revealed that the expression levels of granule component, *Mpo*, *Lactoferrin*, and *Mmp9* were strongly reduced in CD11b$^+$Gr-1$^+$Sca-1$^+$ myeloid cells compared to CD11b$^+$Gr-1$^+$Sca-1$^-$ myeloid cells (Fig. 2F). Together, these results indicate that while both populations of CD11b$^+$Gr-1$^+$ myeloid cells can effectively phagocytose foreign particles, Sca-1$^+$ cells have impaired functional activity in terms of superoxide anion production and degranulation activity.

Myeloid cell–derived cytokines play a critical role in shaping inflammatory responses in vivo (*23*). The basal production of multiple cytokines [interleukin-6 (IL-6), tumor necrosis factor–α (TNFα), interferon-γ (IFN-γ), IL-10] and chemokines (CCL2, CXCL1, and CXCL2) was significantly higher for CD11b$^+$Gr-1$^+$Sca-1$^+$ myeloid cells versus CD11b$^+$Gr-1$^+$Sca-1$^-$ myeloid cells (Fig. 2G, left). To ask whether the increased production of basal levels of cytokines might be due to increased numbers of Sca-1$^+$ versus Sca-1$^-$ CD11b$^+$Gr-1$^+$ myeloid cells, we evaluated survival [propidium iodide (PI)/annexin V staining] and proliferation (Ki67 expression) in the two populations: No significant differences were noted (fig. S3). We also performed intracellular staining for several cytokines and found that CD11b$^+$Gr-1$^+$Sca-1$^+$ cells can produce increased levels of IL-6, TNFα, CCL2, IL-10, and IFN-γ on a per-cell basis (fig. S4). In most cases, lipopolysaccharide (LPS)–stimulated increased production of cytokines/chemokines in both populations of CD11b$^+$Gr-1$^+$ myeloid cells, and LPS-stimulated Sca-1$^+$ myeloid cells secreted significantly more IL-6, CXCL1, IFN-γ, and IL-10 than Sca-1$^-$ myeloid cell comparators (Fig. 2G, right).

IFN-γ is required for the generation of *S. aureus*–induced CD11b$^+$Gr-1$^+$Sca-1$^+$ myeloid cells

Since previous reports demonstrated an important role for IFN-γ in inducing Sca-1 expression by lineage$^-$Sca-1$^-$C-Kit$^+$ cells and lymphocytes (*24*, *25*), we examined the role of IFN-γ on the generation of CD11b$^+$Gr-1$^+$Sca-1$^+$ myeloid cells in the *S. aureus* infection model. Anti–IFN-γ antibody treatment abolished the generation of *S. aureus* infection–induced CD11b$^+$Gr-1$^+$Sca-1$^+$ myeloid cells (Fig. 3A). Similarly, genetic deficiency in *Ifngr1* also completely prevented the generation of infection-induced CD11b$^+$Gr-1$^+$Sca-1$^+$ myeloid cells (Fig. 3B). Previous reports demonstrated that T lymphocytes, monocytes, natural killer (NK) cells, and neutrophils produce IFN-γ in response to pathogen infection (*26*–*29*). We found that *S. aureus* infection caused production of IFN-γ from neutrophils but not T lymphocytes, monocytes, and NK cells in peritoneal exudate (Fig. 3C). In addition, infection-induced generation of CD11b$^+$Gr-1$^+$Sca-1$^+$ myeloid cells was not impaired in Rag$^{-/-}$ mice (fig. S5), further indicating that lymphocytes are dispensable for the in vivo expansion of Sca-1$^+$ myeloid cells. We also tested the effects of IFN-γ on the generation of CD11b$^+$Gr-1$^+$Sca-1$^+$ myeloid cells in vitro. Stimulation of mouse bone marrow cells with IFN-γ increased the population of Sca-1$^+$ myeloid cells, providing additional support for an essential role for IFN-γ in generating CD11b$^+$Gr-1$^+$Sca-1$^+$ myeloid cells (Fig. 3D). We further asked whether IFN-γ stimulated granulocyte-macrophage progenitor (GMP) differentiation to CD11b$^+$Gr-1$^+$Sca-1$^+$ myeloid cells. Addition of IFN-γ to GMPs led to robust myeloid cell differentiation into CD11b$^+$Gr-1$^+$Sca-1$^+$ effectors (Fig. 3E). Together, these results suggest that *S. aureus* infection–induced IFN-γ, likely produced by recruited neutrophils, drives differentiation and expansion of a previously unidentified GMP-derived CD11b$^+$Gr-1$^+$Sca-1$^+$ myeloid cell population.

Depletion of CD11b$^+$Gr-1$^+$Sca-1$^+$ myeloid cells increases survival in an *S. aureus* infection model

To examine the in vivo functional role of CD11b$^+$Gr-1$^+$Sca-1$^+$ myeloid cells in the host response to bacterial infection, we used anti–Sca-1 antibody (clone: E13) to deplete CD11b$^+$Gr-1$^+$Sca-1$^+$ myeloid cells and assessed the effects of depletion on key pathophysiological parameters associated with bacterial infection. Intraperitoneal administration of anti–Sca-1 antibody effectively depleted CD11b$^+$Gr-1$^+$Sca-1$^+$ myeloid cells from peritoneal exudate induced by experimental bacterial infection (Fig. 4A, middle). However, bone marrow cells, which also express Sca-1, were not depleted by intraperitoneal anti–Sca-1 antibody treatment (Fig. 4A, bottom). These results suggest that administration of anti–Sca-1 antibody can be used to isolate the in vivo functional role of CD11b$^+$Gr-1$^+$Sca-1$^+$ myeloid cells recruited into the peritoneum. Depletion of CD11b$^+$Gr-1$^+$Sca-1$^+$ myeloid cells from the peritoneum significantly increased survival following experimentally induced *S. aureus* infection (Fig. 4B). Clinical scores were also significantly improved by anti–Sca-1 antibody administration (Fig. 4D). These results suggest that CD11b$^+$Gr-1$^+$Sca-1$^+$ myeloid cells are pathogenic and cause mortality during bacterial infection. We further investigated the role of CD11b$^+$Gr-1$^+$Sca-1$^+$ myeloid cells in controlling bacterial burden in vivo. Anti–Sca-1 antibody significantly reduced peritoneal exudate CFUs compared with the isotype control (Fig. 4E). We found that administration of anti–Sca-1 antibody significantly increased the number of peritoneal CD11b$^+$Gr-1$^+$Sca-1$^-$ myeloid cells (Fig. 4F). Levels of aspartate aminotransferase (AST) and alanine aminotransferase (ALT), which are biomarkers of vital organ damage, were substantially reduced following anti–Sca-1 treatment, indicating that CD11b$^+$Gr-1$^+$Sca-1$^+$ myeloid cells contribute to host organ damage in vivo (Fig. 4G). *S. aureus* infection also strongly induced lung inflammation, which was markedly blocked by anti–Sca-1 antibody administration but not by the rat immunoglobulin G2a (IgG2a) control (Fig. 4H, top). Anti–Sca-1 antibody administration decreased total protein, cell numbers, and MPO activity in bronchoalveolar lavage fluid (BALF) (Fig. 4H, bottom). Rampant bacterial infection elicits splenocyte apoptosis, which leads to immune paralysis (*30*). Splenocyte apoptosis induced by *S. aureus* infection was significantly inhibited by anti–Sca-1 antibody administration but not by rat IgG2a control (Fig. 4I). The effects of depletion of CD11b$^+$Gr-1$^+$Sca-1$^+$ myeloid cells on the production of cytokines were also tested. Administration of anti–Sca-1 antibody substantially decreased the levels of several cytokines such as IL-6, IL-1β, TNFα, and IFN-γ in peritoneal fluid and serum from *S. aureus*–infected animals compared with controls (Fig. 4J).

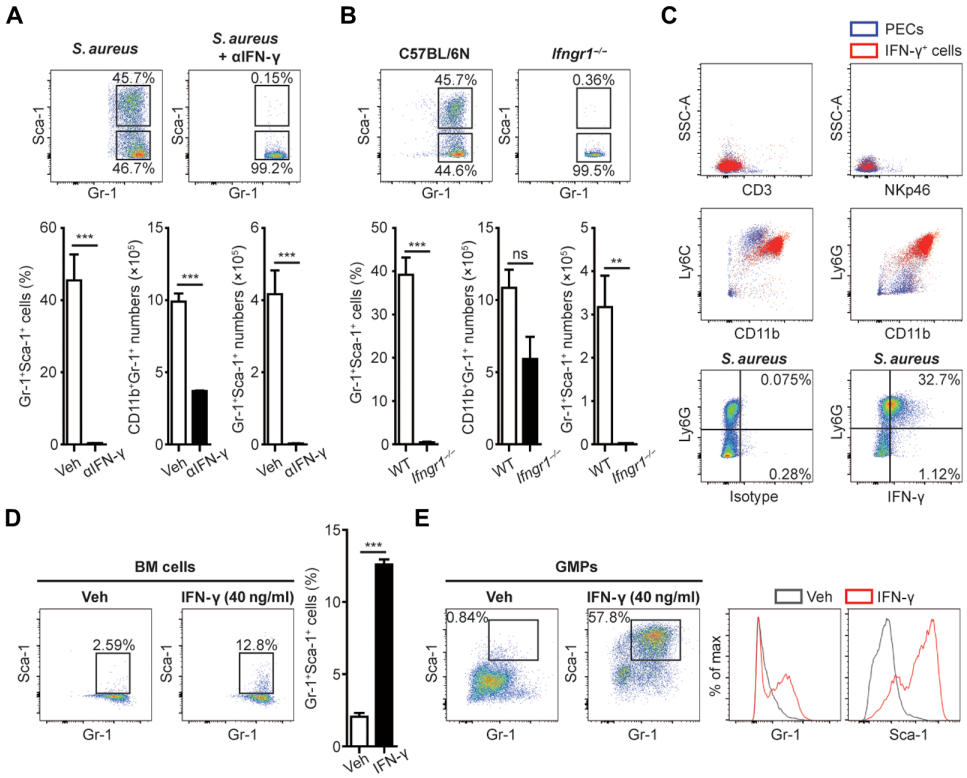

Fig. 3. Essential role of IFN-γ in the generation of CD11b$^+$Gr-1$^+$Sca-1$^+$ myeloid cells in *S. aureus* infection. (**A**) WT mice were injected with anti–IFN-γ antibody (αIFN-γ, 45.45 mg/kg) or isotype control and were infected with *S. aureus* (1×10^7 CFUs per head, intraperitoneal injection). (**B**) WT and *Ifnγr1*$^{-/-}$ mice were infected with *S. aureus* (1×10^7 CFUs per head, intraperitoneal injection). Peritoneal fluids were collected 24 hours after infection, and CD11b$^+$Gr-1$^+$Sca-1$^-$ and CD11b$^+$Gr-1$^+$Sca-1$^+$ myeloid cells were analyzed by flow cytometry (A and B). (**C**) IFN-γ expression on peritoneal exudate cells (PECs) was assessed by intracellular staining. The expression of select surface markers (CD3, NKp46, CD11b, Ly6C, and Ly6G) on either IFN-γ$^+$ cells or IFN-γ$^-$ cells was determined by flow cytometry. (**D**) Bone marrow (BM) cells and (**E**) GMP populations from BM were untreated or stimulated with recombinant IFN-γ (40 ng/ml) for 24 hours. Gr-1 and Sca-1 expression was assessed on CD11b$^+$ cells by flow cytometry (D and E). The data are representative of three independent experiments (A top, B top, C, D left, and E). Data are expressed as means ± SEM ($n = 3$ for A bottom, B bottom, and D right). $^{**}P < 0.01$ and $^{***}P < 0.001$ by Student's *t* test. ns, not significant.

Adoptive transfer of CD11b$^+$Gr-1$^+$Sca-1$^+$ myeloid cells enhanced mortality in an *S. aureus* infection model

To further test whether CD11b$^+$Gr-1$^+$Sca-1$^+$ myeloid cells are pathogenic agents during *S. aureus* infection, we isolated Sca-1$^+$ and Sca-1$^-$ myeloid cells from donor mice and transferred them into the peritoneum of *S. aureus*–infected recipients. Adoptive transfer of Sca-1$^+$ myeloid cells but not Sca-1$^-$ cells significantly enhanced mortality not only in *S. aureus*–infected but also in *E. coli*–infected recipients (Fig. 5A and fig. S6A). Adoptive transfer of Sca-1$^+$ myeloid cells also slightly enhanced mortality in zymosan-injected recipients (fig. S6B). Clinical scores were worse, and CFUs were substantially increased by adoptive transfer of CD11b$^+$Gr-1$^+$Sca-1$^+$ myeloid cells in the infection model (Fig. 5, B and C). Damage of vital organs such as the liver and lung was also enhanced by adoptive transfer of CD11b$^+$Gr-1$^+$Sca-1$^+$ myeloid cells, as evidenced by increased serum AST/ALT levels, and increased protein levels, infiltrating leukocytes, and MPO activity in BALF (Fig. 5, D and E). Splenocyte apoptosis was increased by adoptive transfer of CD11b$^+$Gr-1$^+$Sca-1$^+$ myeloid cells in the model (Fig. 5F). Adoptive transfer of Sca-1$^+$ myeloid cells increased the levels of several proinflammatory cytokines such as IL-6, IL-1β, TNFα, CCL2, and IFN-γ in peritoneal fluid and/or serum (Fig. 5G). Thus, both depletion and transfer studies indicate that host-derived CD11b$^+$Gr-1$^+$Sca-1$^+$ myeloid cells embody pathogenic agents induced by *S. aureus* infection that drive fatal immune dysregulation in vivo.

DISCUSSION

Extreme pathophysiological stressors like tumor or rampant bacterial infection induce expansion of distinct CD11b$^+$Gr-1$^+$ myeloid cell populations (*31*). In this study, we found a previously unidentified population of Sca-1$^+$ myeloid cells generated upon challenge with *S. aureus*, a major clinically relevant Gram-positive bacterium that causes septic shock. Because CD11b$^+$ myeloid cells play essential roles in defending against invading bacterial pathogens, we examined various antibacterial immune defenses commonly used by these acute responder cells. While CD11b$^+$Gr-1$^+$Sca-1$^-$ myeloid cells were well suited for superoxide anion production, their Sca-1$^+$ counterparts were less well equipped, with impaired bacterial killing activity in terms of superoxide anion production and degranulation activity. Depletion of CD11b$^+$Gr-1$^+$Sca-1$^+$ myeloid cells decreased bacterial burden in an *S. aureus* infection model, suggesting that the Sca-1$^+$ myeloid cells suppress the cumulative host-based bacterial killing activity. We next sought to investigate the mechanism of protection following CD11b$^+$Gr-1$^+$Sca-1$^+$ myeloid cell depletion. Unexpectedly, depletion of Sca-1$^+$ myeloid cells significantly augmented the number

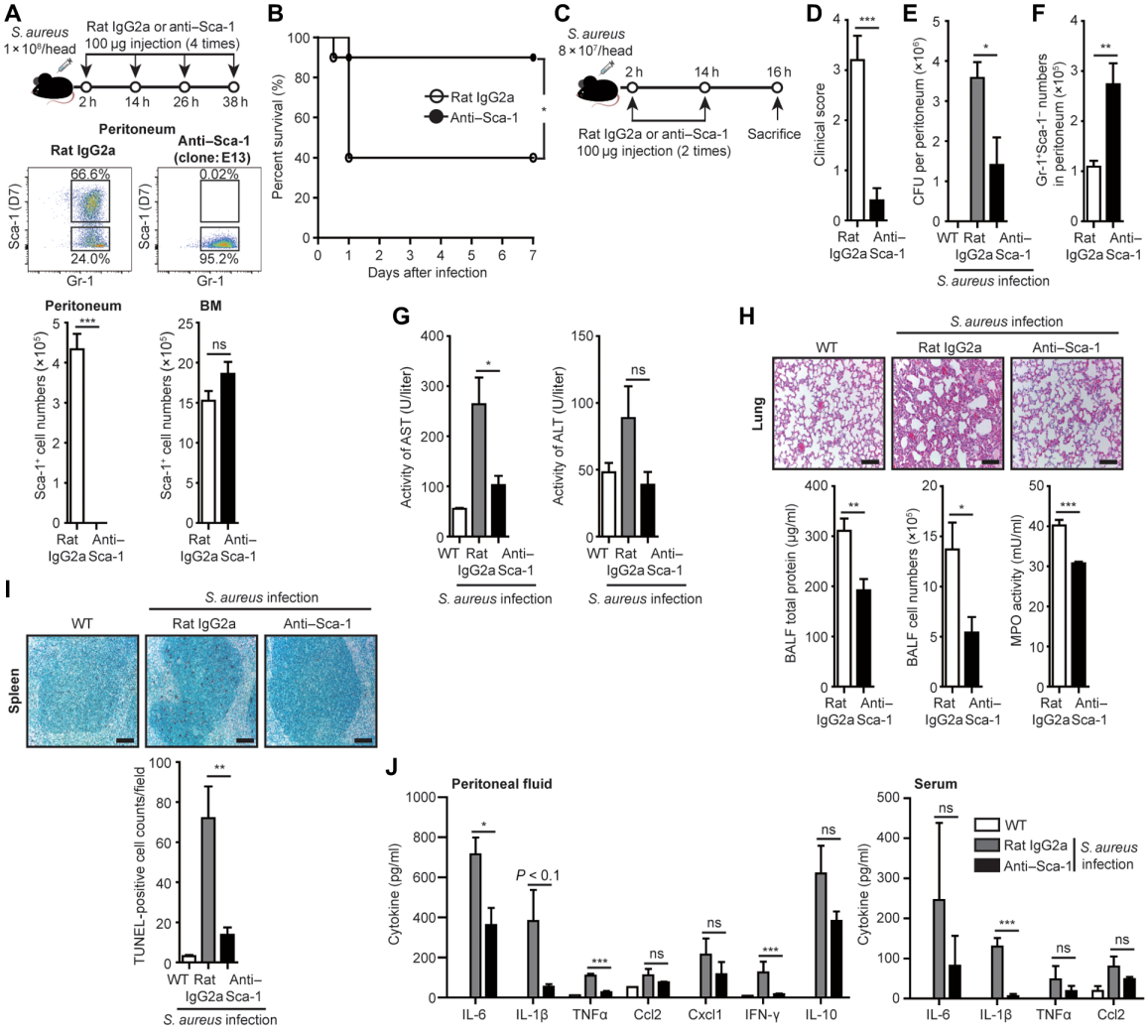

Fig. 4. Effects of CD11b$^+$Gr-1$^+$Sca-1$^+$ cell depletion in *S. aureus* infection. (**A** top and **C**) Depletion protocol to eliminate CD11b$^+$Gr-1$^+$Sca-1$^+$ myeloid cells in vivo with anti–Sca-1 antibody in *S. aureus* infection model for survival data (**B**) and pathology analysis (**D** to **J**). (A middle) Flow cytometry analysis of CD11b$^+$Gr-1$^+$Sca-1$^+$ myeloid cell depletion was assessed 16 hours after infection. (A bottom) The number of CD11b$^+$Gr-1$^+$Sca-1$^+$ cells isolated from the peritoneum and bone marrow of anti–Sca-1–injected mice was compared with isotype control (Rat IgG2a)–injected mice from *S. aureus* (1×10^7 CFUs per head, 16 hours)–infected mice. (B) *S. aureus* (1×10^8 CFUs per head) were injected intraperitoneally with either rat IgG2a (isotype control, 4.55 mg/kg) or anti–Sca-1 antibody (4.55 mg/kg) four times (2, 14, 26, and 38 hours after infection). Survival was monitored for 7 days after infection. (D to J) WT mice were infected with *S. aureus* (8×10^7 CFUs per head) and injected with rat IgG2a (isotype control, 4.55 mg/kg) or anti–Sca-1 antibody (4.55 mg/kg) two times 2 and 14 hours after infection. Mice were euthanized 16 hours after infection. (D) Clinical score was assessed 12 hours after infection. (E) The collected peritoneal fluid samples were cultured overnight on agar plates at 37°C, and CFUs were quantified. (F) Peritoneal CD11b$^+$Gr-1$^+$Sca-1$^-$ myeloid cell number was determined by flow cytometry. (G) Plasma AST and ALT levels were measured by ELISA. (H, top) Lungs were fixed, sectioned, and stained with hematoxylin and eosin. (H bottom) Protein level, recruited cell numbers, and MPO activity were analyzed from BALF. (I) A TUNEL assay to determine splenocyte apoptosis was performed on fixed tissue sections, and TUNEL-positive cells were quantified (I bottom). (J) Cytokine levels were measured by ELISA. Scale bars, 100 μm (H top and I top). The data are representative of three independent experiments (A middle, H top, and I top). Sample size: $n = 20$ per group (B). Data are expressed as means ± SEM ($n = 5$ for A bottom, D, E, F, G, H bottom, I bottom, and J). Statistical significance was determined by log-rank test (B). *$P < 0.05$, **$P < 0.01$, and ***$P < 0.001$ by Student's t test. ns, not significant.

of peritoneal Sca-1$^-$ myeloid cells (Fig. 4F). Given their increased capacity for bacterial killing, increased numbers of Sca-1$^-$ myeloid cells may underlie the protective effects of Sca-1$^+$ myeloid cell depletion in our studies.

Previous reports describe expansion of MDSCs from bacteria-infected or tumor-bearing mice (*31*, *32*). CD11b$^+$Gr-1$^+$Sca-1$^+$ myeloid cells are distinct from MDSCs in the following characteristics: (i) CD11b$^+$Gr-1$^+$Sca-1$^+$ myeloid cells have different immunophenotypes, e.g., they do not express of Ly6G (very low expression for Ly6C), CD115, and F4/80, which are phenotypic markers of polymorphonuclear (PMN)–MDSCs or monocytic (M)–MDSCs (*33*). (ii) CD11b$^+$Gr-1$^+$Sca-1$^+$ myeloid cells do not show suppressive effects on αCD3/CD28 T cell activation. (iii) CD11b$^+$Gr-1$^+$Sca-1$^+$ myeloid cells produce low levels of reactive oxygen species. (iv) CD11b$^+$Gr-1$^+$Sca-1$^+$ myeloid cells are not detected either in a tumor (as a tumor-infiltrating leukocyte) or in the blood of tumor-bearing mice (B16 melanoma model). Given these different characteristics, CD11b$^+$Gr-1$^+$Sca-1$^+$ myeloid cells seem to be pathologically activated immature myeloid cells distinct from MDSCs generated in response to bacterial infection. Since CD11b$^+$Gr-1$^+$Sca-1$^+$ myeloid cells express slightly

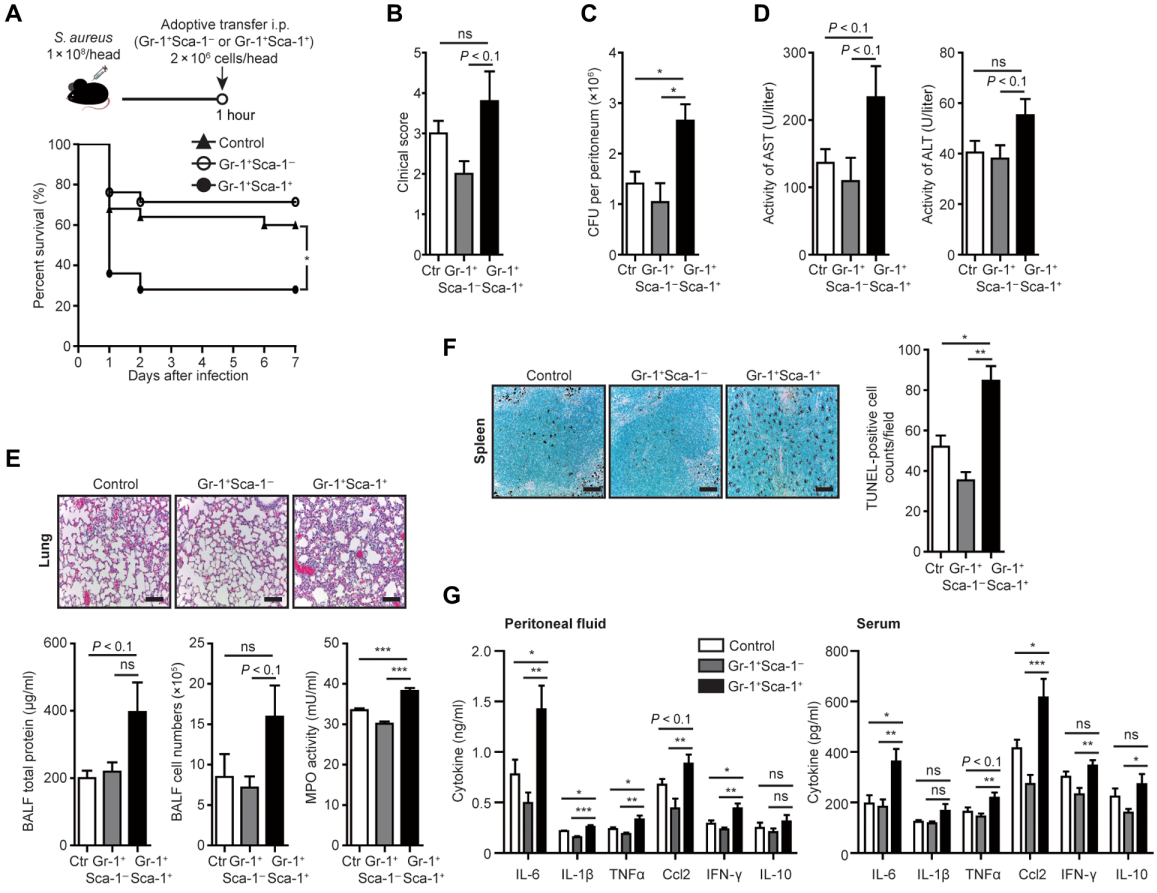

Fig. 5. Pathogenic role of CD11b$^+$Gr-1$^+$Sca-1$^+$ myeloid cells in *S. aureus*–infected mice. (**A** top) Model protocol to adoptively transfer CD11b$^+$Gr-1$^+$Sca-1$^-$ or CD11b$^+$Gr-1$^+$Sca-1$^+$ myeloid cells intraperitoneally into *S. aureus*–infected mice. (A bottom) Survival was monitored for 7 days after infection. i.p., intraperitoneally. (**B** to **G**) WT mice were infected with *S. aureus* (8×10^7 CFUs per head) and euthanized 16 hours after infection. (B) Clinical score was assessed 12 hours after infection. (C) The collected peritoneal fluid samples were cultured overnight on agar plates at 37°C, and CFUs were quantified. (D) Plasma AST and ALT levels were measured by ELISA. (E top) Lungs were fixed, sectioned, and stained with hematoxylin and eosin. (E bottom) Protein level, recruited cell numbers, and MPO activity were analyzed from BALF. (F left) A TUNEL assay to determine splenocyte apoptosis was performed on fixed tissue sections, and TUNEL-positive cells were quantified (F right). (G) Cytokine levels were measured by ELISA. Scale bars, 100 μm (E top and F left). Ctr, control. The data are representative of three independent experiments (E top and F left). Data are expressed as means ± SEM ($n = 10$ for B to D, E bottom, F right, and G). Sample size: $n = 20$ mice per group (A). Statistical significance was determined by log-rank test (A). *$P < 0.05$, **$P < 0.01$, and ***$P < 0.001$ by Student's *t* test. ns, not significant.

higher levels of monocyte-associated markers (Ly6C, CCR2, and CX3CR1) but do not express the key monocytic cell lineage marker (CD115), and CD11b$^+$Gr-1$^+$Sca-1$^-$ myeloid cells express high levels of neutrophil-associated markers (Ly6G, CXCR2, and CD101), we conclude that CD11b$^+$Gr-1$^+$Sca-1$^+$ cells comprise a population of uncommitted myeloid cell precursors and that CD11b$^+$Gr-1$^+$Sca-1$^-$ cells comprise a population of neutrophil lineage cells. This is further supported by the Giemsa staining analysis, which shows distinct nuclear morphologies and nucleus-to-cytoplasm ratios in line with our immunophenotyping results.

In studies investigating the mechanism underlying the generation of CD11b$^+$Gr-1$^+$Sca-1$^+$ myeloid cells, we found that IFN-γ plays an indispensable role in vivo as well as in vitro. Depletion of IFN-γ using anti–IFN-γ antibody, or genetic deficiency in *Ifngr1*, significantly inhibited the generation of *S. aureus*–induced CD11b$^+$Gr-1$^+$ Sca-1$^+$ myeloid cells (Fig. 3, A and B). In vitro stimulation of bone marrow cells with purified IFN-γ increased the generation of CD11b$^+$ Gr-1$^+$Sca-1$^+$ myeloid cells (Fig. 3D). Bone marrow–derived GMPs stimulated with IFN-γ efficiently differentiated into CD11b$^+$Gr-1$^+$ Sca-1$^+$ myeloid cells (Fig. 3E). These results suggest that bone marrow GMPs are developmental progenitors of CD11b$^+$Gr-1$^+$Sca-1$^+$ myeloid cells. Previous studies demonstrated a crucial role for IFN-γ in the expression of Sca-1 in T cells, monocytes, and Lin$^-$Sca-1$^+$C-Kit$^+$ cells (*18*, *25*, *34*). Since IFN-γ is indispensable in generating CD11b$^+$ Gr-1$^+$Sca-1$^+$ myeloid cells, we sought to identify the cells that produce IFN-γ in the *S. aureus* infection model. Intracellular staining for IFN-γ by several different leukocytes (T lymphocytes, NK cells, monocytes, and neutrophils) from peritoneal exudate revealed that only neutrophils produced IFN-γ in the experimental infection model system (Fig. 3C). Recruited peritoneal neutrophils produced IFN-γ, and thus, we hypothesize that neutrophil-derived IFN-γ provides paracrine stimulation to generate CD11b$^+$Gr-1$^+$Sca-1$^+$ myeloid cells. Since CD11b$^+$Gr-1$^+$Sca-1$^+$ myeloid cells show immature functional activity compared to their Sca-1$^-$ counterparts, we asked whether CD11b$^+$Gr-1$^+$Sca-1$^+$ cells could differentiate into CD11b$^+$Gr-1$^+$Sca-1$^-$ cells in response to granulocyte colony-stimulating factor (G-CSF) or other infection-mimicking stimuli such as LPS or *S. aureus*. CD11b$^+$ Gr-1$^+$Sca-1$^+$ cells did not differentiate into CD11b$^+$Gr-1$^+$Sca-1$^-$ cells

under these conditions, suggesting that CD11b$^+$Gr-1$^+$Sca-1$^+$ cells are not precursors of CD11b$^+$Gr-1$^+$Sca-1$^-$ cells (fig. S7). It has been reported that diverse virulent factors produced by *S. aureus* can lead to inflammation and immune cell dysfunction in infected hosts (*35*). While additional experiments are needed to identify the role of discrete virulence factors in the generation of pathogenic CD11b$^+$Gr-1$^+$Sca-1$^+$ cells under *S. aureus* infection, our findings on the effects of heat-killed *S. aureus* and LTA in the generation of CD11b$^+$Gr-1$^+$Sca-1$^+$ cells suggest that heat-resistant molecules including LTA would be one of the active components involved in the pathomechanism.

In vitro analysis revealed that CD11b$^+$Gr-1$^+$Sca-1$^+$ myeloid cells have generally impaired migratory activity toward chemoattractants/chemokines (Fig. 2B). However, CD11b$^+$Gr-1$^+$Sca-1$^+$ myeloid cells produced increased levels of proinflammatory cytokines that contribute to systemic inflammation in the experimental infection model (Fig. 2G). To understand the in vivo functional role of CD11b$^+$Gr-1$^+$Sca-1$^+$ myeloid cells during *S. aureus* infection, we established two different systems: depletion of the Sca-1$^+$ myeloid cells using anti–Sca-1 antibodies and adoptive transfer of Sca-1$^+$ or Sca-1$^-$ myeloid cells. Local intraperitoneal administration of anti–Sca-1 antibodies selectively depleted peritoneal CD11b$^+$Gr-1$^+$Sca-1$^+$ myeloid cells without affecting the abundance of bone marrow cells that express Sca-1 (Fig. 4A). Depletion of CD11b$^+$Gr-1$^+$Sca-1$^+$ myeloid cells substantially decreased liver and lung inflammation, splenocyte apoptosis, and the production of inflammatory cytokines, ultimately leading to increased survival rates in response to *S. aureus* challenge (Fig. 4, B and D to J). On the other hand, adoptive transfer of CD11b$^+$Gr-1$^+$Sca-1$^+$ myeloid cells into *S. aureus*–challenged mice enhanced the lethality of the bacterial infection (Fig. 5). Adoptive transfer of CD11b$^+$Gr-1$^+$Sca-1$^+$ myeloid cells also enhanced mortality in *E. coli*– or zymosan-challenged mice (fig. S6). These results suggest that CD11b$^+$Gr-1$^+$Sca-1$^+$ myeloid cells play an essential pathogenic role during bacterial (both of Gram-positive and Gram-negative) or yeast infection. Since CD11b$^+$Gr-1$^+$Sca-1$^+$ myeloid cells have impaired innate defense activity as well as increased inflammatory cytokine production, these effects are likely additive if not synergistic and contribute in aggregate to the observed augmented mortality.

In conclusion, in this study we found that experimental *S. aureus* infection generated a previously unidentified pathogenic myeloid cell population that expresses Sca-1. This newly characterized myeloid cell population is abundantly generated in response to bacterial infection and produces comparatively higher levels of proinflammatory cytokines and chemokines than their Sca-1–negative counterparts, but fails to produce superoxide anion and contributes substantially to mortality in an in vivo model of bacterial infection. Our finding provides unique insight into a new myeloid cell population that drives the pathomechanism of disease during severe bacterial infection.

MATERIALS AND METHODS

Mice

WT C57BL/6N male mice, 8 weeks old, were purchased from Orient Bio Inc. (Seongnam, Korea). All animal experiments were performed in accordance with the Korea Food and Drug Administration guidelines. Protocols were approved by the Institutional Review Committee for Animal Care and Use at Sungkyunkwan University (Suwon, Korea). The *Rag*$^{-/-}$ mice were gifted by Y. S. Bae (Sungkyunkwan University, Suwon, Korea), and the *Ifngr1*$^{-/-}$ mice were gifted by S. J. Ha (Yonsei University, Seoul, Korea).

Antibodies and flow cytometry analysis

Antibodies to CD11b (M1/70), Gr-1 (RB6-8C5), Sca-1 (D7), NKp46 (29A1.4), CD3 (145-2C11), CD115 (AFS98), CD101 (Moushi101), Ly6C (HK1.4), CD34 (RAM34), F4/80 (BM8), CD11c (N418), CD19 (eBio103), Siglec-F (E50-2440), Ly6G (1A8), Ki67 (SolA15), annexin V, and PI were purchased from Thermo Fisher Scientific (Waltham, MA, USA). Antibodies to CCR2 (SA203G11) and CX3CR1 (SA011F11) were purchased from BioLegend (San Diego, CA, USA), and to CXCR2 (242216) were from R&D systems Inc. (Minneapolis, MN, USA). Receptor expression was analyzed using a BD FACS Canto II flow cytometer and FlowJo analytical software (BD Biosciences, San Jose, CA, USA).

Staining of intracellular cytokine

Immune cells collected from *S. aureus* (1×10^7 CFUs per head)–infected mice were incubated with brefeldin A solution for 3 hours at 37°C in a round-shaped 96-well microplate. After adding BD GolgiStop, cells were stained with fixable viability dye for 30 min. For the measurement of surface expression of immune cell markers, cells were stained for 45 min after Fc blocking at 4°C. Stained cells were fixed with intracellular (IC) fixation buffer for 30 min and permed for 20 min at room temperature. Then, permed cells were stained with phycoerythrin (PE)–conjugated anti–IFN-γ (BD Biosciences, San Jose, CA, USA), anti–IL-6, anti–IL-10, anti-TNFα (Thermo Fisher Scientific, Waltham, MA, USA), and anti-CCL2 (BioLegend, San Diego, CA, USA) for 1 hour. Data were analyzed using a BD FACS Canto II flow cytometer and FlowJo analytical software (BD Biosciences, San Jose, CA, USA).

Sorting of mouse CD11b$^+$Gr-1$^+$ cells from bacterial infection models

WT C57BL/6N male mice (8 weeks old) were infected with *S. aureus* (1×10^7 CFUs per head). Mouse peritoneal cells were collected at 24 hours after model establishment, and CD11b$^+$Gr-1$^+$Sca-1$^-$ and CD11b$^+$Gr-1$^+$Sca-1$^+$ cells were sorted using a BD FACSaria III (BD Biosciences, San Jose, CA, USA).

In vivo inflammatory models

WT C57BL/6N male mice (8 weeks old) were infected with *S. aureus* (1×10^7 CFUs per head) or *E. coli* (5×10^6 CFUs per head) by intraperitoneal injection. Other mice were injected with LTA (6 mg/kg) or zymosan (45.45 mg/kg). Mouse peritoneal cells were collected at 24 hours after model establishment. LTA from *S. aureus* and zymosan A from *Saccharomyces cerevisiae* were purchased from Sigma-Aldrich (St. Louis, MO, USA).

Bacterial strains and growth conditions

S. aureus strain type ATCC 25923 and *E. coli* strain type BL21-DE3 were obtained from the American Type Culture Collection (ATCC) (Manassas, VA, USA). *S. aureus* cultures were grown for 12 hours at 37°C in tryptic soy broth (Difco Laboratories, Detroit, MI, USA). *E. coli* cultures were grown for 12 hours at 37°C in LB broth (Duchefa Biochemie, BH Haarlem, The Netherlands). Live *S. aureus* and *E. coli* bacteria at stationary stage were collected and resuspended in sterile phosphate-buffered saline.

Measurement of superoxide anion

Superoxide anion generation was measured by the cytochrome c reduction assay. Sorted CD11b$^+$Gr-1$^+$Sca-1$^-$ and CD11b$^+$Gr-1$^+$Sca-1$^+$ myeloid cells were stimulated with PMA (1 μM). Superoxide anion generation was measured according to a previous report (*36*).

Giemsa staining

Sorted CD11b$^+$Gr-1$^+$Sca-1$^-$ and CD11b$^+$Gr-1$^+$Sca-1$^+$ myeloid cells were centrifuged for 3 min at 500 rpm and then stained with Giemsa stain solutions from Sigma-Aldrich (St. Louis, MO, USA) for 7 min. Images were acquired using a Leica DM750 light microscope.

Reverse transcription quantitative polymerase chain reaction analysis

Quantitative polymerase chain reaction (qPCR) was designed on the basis of consensus sequences of each alignment and performed using the Rotor-Gene Q (2plex on PC) instrument from QIAGEN (Hilden, Germany) with SYBR Green qPCR Mix (Biofact, Daejeon, Korea). RNA was extracted from sorted CD11b$^+$Gr-1$^+$Sca-1$^-$ and CD11b$^+$Gr-1$^+$Sca-1$^+$ myeloid cells with TRIzol Reagent from Life Technology (Carlsbad, CA, USA). The Maxime RT Premix purchased from iNtRON Biotechnology (Seongnam, Korea) was used to generate cDNA following the manufacturer's directions. The following primers were used for qPCR: *Fpr1*-forward, 5′-CACAATCCAAGTCCGTGAACG-3′; *Fpr1*-reverse, 5′-CAGCTGTTGAAGAAAGCCAAGG-3′; *Fpr2*-forward, 5′-GTCAAGATCAACAGAAGAAACC-3′; *Fpr2*-reverse, 5′-GGGCTCTCTCAAGACTATAAGG-3′; *Cxcr1*-forward, 5′-AATCTGTTGTGGCTTCACCCA-3′; *Cxcr1*-reverse, 5′-GCTATCTTCCGCCAGGCATAT-3′; *Cxcr2*-forward, 5′-AGCAAACACCTCTACTACCCTCTA-3′; *Cxcr2*-reverse, 5′-GGGCTGCATCAATTCAAATACCA-3′; *C5ar*-forward, 5′-CAAGACGCTCAAAGTGGTGA-3′; *C5ar*-reverse, 5′-TATGATGCTGGGGAGAGACC-3′; *Nox1*-forward, 5′-CTCCCTTTGCTTCCATCTTG-3′; *Nox1*-reverse, 5′-CCAGCCAGTGAGGAAGAGAC-3′; *Nox2*-forward, 5′-CAAGATGGAGGTGGGACAGT-3′; *Nox2*-reverse, 5′-GCTTATCACAGCCACAAGCA-3′; *Nox4*-forward, 5′-ATCTTTGCCTCGAGGGTTTT-3′; *Nox4*-reverse, 5′-TGACAGGTTTGTTGCTCCTG-3′; *P67 phox*–forward, 5′-GCAGTGGCCTACTTCCAGAG-3′; *P67 phox*–reverse, 5′-GCTCGGACTTCATGTTGGTT-3′; *Mpo*-forward, 5′-ACCTACCCCAGTACCGATCC-3′; *Mpo*-reverse, 5′-AACTCTCCAGCTGGCAAAAA-3′; *Lactoferrin*-forward, 5′-ACCGCAGGCTGGAACATC-3′; *Lactoferrin*-reverse, 5′-CACCCTTCTCATCACCAATACAC-3′; *Mmp9*-forward, 5′-ATAGAGGAAGCCCATTACAGG-3′; *Mmp9*-reverse, 5′-GTGTACACCCACATTTGACG-3′;

Gapdh-forward, 5′-TCCACCACCCTGTTGCTGTA-3′; and *Gapdh*-reverse, 5′-AATGTGTCCGTCGTGGATCT-3′. For qPCR, 40 PCR cycles were performed at 94°C (denaturation, 30 s), 60°C (annealing, 30 s), and 72°C (extension, 1 min). The qPCR data were normalized by using the $2^{-(\Delta\Delta Ct)}$ method against the expression of *Gapdh* as an internal control for calculation of ΔCt values for each gene.

Transcriptome profiling

Total RNA was measured for transcript expression by transcriptome analysis using the HiSeq 4000 Sequencing Reagent Kit. The whole transcriptome expression data from the CD11b$^+$Gr-1$^+$Sca-1$^-$ and CD11b$^+$Gr-1$^+$Sca-1$^+$ myeloid cells were analyzed in Macrogen Inc. (Seoul, Korea).

Phagocytosis assay

Sorted CD11b$^+$Gr-1$^+$Sca-1$^-$ and CD11b$^+$Gr-1$^+$Sca-1$^+$ myeloid cells were incubated with GFP–*E. coli*, fluorescein isothiocyanate–*S. aureus*, or PE-latex beads for 2 hours at 37°C in 5% CO_2 in RPMI 1640 medium. After incubation, samples were examined for the uptake of fluorescently labeled probes by a BD FACS Canto II flow cytometer.

Western blot

Cell lysates were prepared by adding two times Laemmli sample buffer to sorted CD11b$^+$Gr-1$^+$Sca-1$^-$ and CD11b$^+$Gr-1$^+$Sca-1$^+$ myeloid cells. The protein samples were resolved on 10 or 12% SDS–polyacrylamide gel electrophoresis gels and transferred to polyvinylidene difluoride membranes. Membranes were blocked in 4% bovine serum albumin in TBS-T for 1 hour at room temperature. Primary antibodies used were anti–Sca-1 (1:2000) from Abcam (Cambridge, MA, USA) and anti–β-actin (1:2500) from Cell Signaling Technology (Beverly, MA, USA). Secondary horseradish peroxidase–conjugated antibodies used were anti-mouse IgG and anti-rabbit IgG (all 1:5000) from Enzo Lifesciences (Farmingdale, NY, USA).

In vivo administration of anti–Sca-1 antibody

To examine the function of CD11b$^+$Gr-1$^+$Sca-1$^+$ myeloid cells in vivo, purified anti–Sca-1 antibody (clone: E13-161.7) purchased from BioLegend (San Diego, CA, USA) was used. WT mice were infected with a lethal dose of *S. aureus* (1×10^8 CFUs per head), and then, anti–Sca-1 antibody (4.55 mg/kg) or isotype control was intraperitoneally injected for four times at 2, 14, 26, and 38 hours after *S. aureus* infection. We assessed the clinical score 12 hours after infection. The symptoms of the score include mice appearance, behavior, clinical signs, and hydration status. We determined survival rate daily for 7 days after infection.

Adoptive transfer model

The CD11b$^+$Gr-1$^+$Sca-1$^-$ and CD11b$^+$Gr-1$^+$Sca-1$^+$ myeloid cells were sorted from the peritoneum of *S. aureus* (1×10^7 CFUs per head)–infected mice. Isolated cells (2×10^6) were injected into the peritoneum of mouse after *S. aureus* infection (1×10^8 CFUs per head for survival experiment, 8×10^7 CFUs per head for pathomechanism analysis), *E. coli* infection (3×10^8 CFUs per head), or zymosan injection (2 g/kg).

In vivo blockade of IFN-γ

S. aureus (1×10^7 CFUs per head)–infected mice were administered αIFN-γ (R4-6A2, 45.45 mg/kg) or isotype control purchased from Bio X Cell (Lebanon, NH, USA) by intraperitoneal injection once at 1 hour after *S. aureus* infection. Mice were euthanized 24 hours after *S. aureus* infection.

In vitro stimulation of cells with recombinant IFN-γ

Bone marrow cells (1×10^6 cells) or GMP populations (1×10^5 cells) were stimulated with recombinant IFN-γ (40 ng/ml) for 24 hours at 37°C in 5% RPMI 1640 medium. Stimulated cells were stained with anti-CD11b, anti–Gr-1, and anti–Sca-1.

Measurement of cytokines and chemokines

Levels of cytokine and chemokine were measured by enzyme-linked immunosorbent assay (ELISA) using antibody pairs or kits from Thermo Fisher Scientific (Waltham, MA, USA) according to the manufacturer's instructions.

Chemotaxis assay

Sorted CD11b$^+$Gr-1$^+$Sca-1$^-$ and CD11b$^+$Gr-1$^+$Sca-1$^+$ myeloid cells were placed onto the upper well of a chamber separated by a 3-μm polyhydrocarbon filter (Neuro Probe Inc., Gaithersburg, MD, USA) from an fMLF (1 μM)–, WKYMVm (1 μM)–, C5a (10 ng/ml)–, or CXCL2 (30 ng/ml)–containing lower well. Chemotaxis assays were performed according to a previous report (*37*).

Degranulation assay

Sorted CD11b$^+$Gr-1$^+$Sca-1$^-$ and CD11b$^+$Gr-1$^+$Sca-1$^+$ myeloid cells were stimulated with PMA (1 μM) for 30 min at 37°C. Release of secretory granules contents was determined using the β-hexosaminidase assay (*38*).

Determination of bacterial counts

Bacterial counts were determined from peritoneal lavage fluids collected 16 hours after *S. aureus* infection. Collected peritoneal fluids were diluted to 1:1000 and 1:10,000, plated on tryptic soy agar dishes (Difco Laboratories, Detroit, MI, USA), and incubated for 24 hours at 37°C. Bacterial counts were determined according to a previous report (*39*).

Measurement of serum AST and ALT levels

The AST and ALT levels of serum were measured using commercially available kits from Sigma-Aldrich (St. Louis, MO, USA) according to standard laboratory techniques (*40*).

Measurement of protein and MPO activity from BALF

BALF of mice was collected with 900 μl of cold phosphate-buffered saline. BALF sample was used to quantify the total protein level by BCA protein assay kit from Thermo Fisher Scientific (Waltham, MA, USA). MPO activity was measured using the MPO activity assay kit from Abcam (Cambridge, MA, USA).

Hematoxylin and eosin staining and TUNEL assay

The lungs and spleens from mice were harvested in a steady state or 16 hours after *S. aureus* infection for paraffin sectioning. The tissues were fixed in 10% formalin for 24 hours at room temperature and were embedded into paraffin and cut into 4-μm-thick slices, deparaffinized, and rehydrated using xylene, ethanol, and water by standard methods. For the TUNEL (terminal deoxynucleotidyl transferase–mediated deoxyuridine triphosphate nick end labeling) assay, the sections were permeabilized with Triton X-100 at 4°C for 2 min and flooded with the In Situ Cell Death Detection Kit (Roche; 11684795910) for 60 min at 37°C. Hematoxylin and eosin staining and TUNEL assay were conducted according to a previous report (*39*).

Statistical analysis

All results are expressed as the means ± SEM for the data obtained from the indicated number of experiments. Statistical analysis was performed using Student's *t* test or two-way analysis of variance (ANOVA). Survival data were analyzed using the log-rank test. A P value ≤ 0.05 was considered statistically significant.

SUPPLEMENTARY MATERIALS

Supplementary material for this article is available at http://advances.sciencemag.org/cgi/content/full/6/4/eaax8820/DC1

Supplementary Materials and Methods

Fig. S1. CD11b$^+$Gr-1$^+$Sca-1$^+$ myeloid cells are increased in pathologic conditions including *S. aureus* infection.

Fig. S2. CD11b$^+$Gr-1$^+$Sca-1$^-$ and CD11b$^+$Gr-1$^+$Sca-1$^+$ myeloid cells have similar phagocytic activity.

Fig. S3. Survival and proliferation of CD11b$^+$Gr-1$^+$Sca-1$^-$ and CD11b$^+$Gr-1$^+$Sca-1$^+$ myeloid cells are similar.

Fig. S4. CD11b$^+$Gr-1$^+$Sca-1$^+$ myeloid cells produce more cytokines than CD11b$^+$Gr-1$^+$Sca-1$^-$ myeloid cells.

Fig. S5. *S. aureus* infection–induced generation of CD11b$^+$Gr-1$^+$Sca-1$^+$ myeloid cells is not impaired in Rag$^{-/-}$ mice.

Fig. S6. Pathogenic role of CD11b$^+$Gr-1$^+$Sca-1$^+$ myeloid cells in *E. coli*–infected or zymosan-injected mice.

Fig. S7. CD11b$^+$Gr-1$^+$Sca-1$^+$ myeloid cells cannot give rise to CD11b$^+$Gr-1$^+$Sca-1$^-$ myeloid cells.

Data file S1. Transcriptome analysis of the CD11b$^+$Gr-1$^+$Sca-1$^-$ and CD11b$^+$Gr-1$^+$Sca-1$^+$ myeloid cells.

View/request a protocol for this paper from *Bio-protocol*.

REFERENCES AND NOTES

1. O. Soehnlein, L. Lindbom, Phagocyte partnership during the onset and resolution of inflammation. *Nat. Rev. Immunol.* **10**, 427–439 (2010).
2. C. Nathan, Neutrophils and immunity: Challenges and opportunities. *Nat. Rev. Immunol.* **6**, 173–182 (2006).
3. D. F. Bainton, J. L. Ullyot, M. G. Farquhar, The development of neutrophilic polymorphonuclear leukocytes in human bone marrow. *J. Exp. Med.* **134**, 907–934 (1971).
4. C. Shi, E. G. Pamer, Monocyte recruitment during infection and inflammation. *Nat. Rev. Immunol.* **11**, 762–774 (2011).
5. Y.-W. Yang, W.-H. Luo, Recruitment of bone marrow CD11b$^+$Gr-1$^+$ cells by polymeric nanoparticles for antigen cross presentation. *Sci. Rep.* **7**, 44691 (2017).
6. J. M. Daley, A. A. Thomay, M. D. Connolly, J. S. Reichner, J. E. Albina, Use of Ly6G-specific monoclonal antibody to deplete neutrophils in mice. *J. Leukoc. Biol.* **83**, 64–70 (2008).
7. J. W. Tam, A. L. Kullas, P. Mena, J. B. Bliska, A. W. M. van der Velden, CD11b$^+$ Ly6C^{hi} Ly6G- immature myeloid cells recruited in response to *Salmonella enterica* serovar Typhimurium infection exhibit protective and immunosuppressive properties. *Infect. Immun.* **82**, 2606–2614 (2014).
8. L. Yang, L. M. DeBusk, K. Fukuda, B. Fingleton, B. Green-Jarvis, Y. Shyr, L. M. Matrisian, D. P. Carbone, P. C. Lin, Expansion of myeloid immune suppressor Gr$^+$CD11b$^+$ cells in tumor-bearing host directly promotes tumor angiogenesis. *Cancer Cell* **6**, 409–421 (2004).
9. V. Bronte, S. Brandau, S.-H. Chen, M. P. Colombo, A. B. Frey, T. F. Greten, S. Mandruzzato, P. J. Murray, A. Ochoa, S. Ostrand-Rosenberg, P. C. Rodriguez, A. Sica, V. Umansky, R. H. Vonderheide, D. I. Gabrilovich, Recommendations for myeloid-derived suppressor cell nomenclature and characterization standards. *Nat. Commun.* **7**, 12150 (2016).
10. S. A. Kusmartsev, Y. Li, S.-H. Chen, Gr-1$^+$ Myeloid cells derived from tumor-bearing mice inhibit primary T cell activation induced through CD2/CD28 costimulation. *J. Immunol.* **165**, 779–785 (2000).
11. X. Song, Y. Krelin, T. Dvorkin, O. Bjorkdahl, S. Segal, C. A. Dinarello, E. Voronov, R. N. Apte, CD11b$^+$/Gr-1$^+$ immature myeloid cells mediate suppression of T cells in mice bearing tumors of IL-1β-secreting cells. *J. Immunol.* **175**, 8200–8208 (2005).
12. Q. Li, P.-Y. Pan, P. Gu, D. Xu, S.-H. Chen, Role of immature myeloid Gr-1$^+$ cells in the development of antitumor immunity. *Cancer Res.* **64**, 1130–1139 (2004).
13. L. Yang, C. M. Edwards, G. R. Mundy, Gr-1$^+$CD11b$^+$ myeloid-derived suppressor cells: Formidable partners in tumor metastasis. *J. Bone Miner. Res.* **25**, 1701–1706 (2010).
14. S. Xia, H. Sha, L. Yang, Y. Ji, S. Ostrand-Rosenberg, L. Qi, Gr-1$^+$CD11b$^+$ myeloid-derived suppressor cells suppress inflammation and promote insulin sensitivity in obesity. *J. Biol. Chem.* **286**, 23591–23599 (2011).
15. G. J. Spangrude, S. Heimfeld, I. L. Weissman, Purification and characterization of mouse hematopoietic stem cells. *Science* **241**, 58–62 (1988).
16. M. Niederquell, S. Kurig, J. A. A. Fischer, S. Tomiuk, M. Swiecki, M. Colonna, I. C. D. Johnston, A. Dzionek, Sca-1 expression defines developmental stages of mouse pDCs that show functional heterogeneity in the endosomal but not lysosomal TLR9 response. *Eur. J. Immunol.* **43**, 2993–3005 (2013).
17. H.-C. Chen, F. Frissora, J. E. Durbin, N. Muthusamy, Activation induced differential regulation of stem cell antigen-1 (Ly-6A/E) expression in murine B cells. *Cell. Immunol.* **225**, 42–52 (2003).
18. M. H. Askenase, S.-J. Han, A. L. Byrd, D. Morais da Fonseca, N. Bouladoux, C. Wilhelm, J. E. Konkel, T. W. Hand, N. Lacerda-Queiroz, X.-z. Su, G. Trinchieri, J. R. Grainger, Y. Belkaid, Bone-marrow-resident NK cells prime monocytes for regulatory function during infection. *Immunity* **42**, 1130–1142 (2015).
19. M. Evard, I. W. H. Kwok, S. Z. Chong, K. W. W. Teng, E. Becht, J. Chen, J. L. Sieow, H. L. Penny, G. C. Ching, S. Devi, J. M. Adrover, J. L. Y. Li, K. H. Liong, L. Tan, Z. Poon, S. Foo, J. W. Chua, I.-H. Su, K. Balabanian, F. Bachelerie, S. K. Biswas, A. Larbi, W. Y. K. Hwang, V. Madan, H. P. Koeffler, S. C. Wong, E. W. Newell, A. Hidalgo, F. Ginhoux, L. G. Ng, Developmental analysis of bone marrow neutrophils reveals populations specialized in expansion, trafficking, and effector functions. *Immunity* **48**, 364–379 (2018).
20. T. N. Mayadas, X. Cullere, C. A. Lowell, The multifaceted functions of neutrophils. *Annu. Rev. Pathol.* **9**, 181–218 (2014).
21. C. C. Winterbourn, A. J. Kettle, M. B. Hampton, Reactive oxygen species and neutrophil function. *Annu. Rev. Biochem.* **85**, 765–792 (2016).
22. M. Faurschou, N. Borregaard, Neutrophil granules and secretory vesicles in inflammation. *Microbes Infect.* **5**, 1317–1327 (2003).
23. C. Tecchio, A. Micheletti, M. A. Cassatella, Neutrophil-derived cytokines: Facts beyond expression. *Front. Immunol.* **5**, 508 (2014).

24. P. Zhang, S. Nelson, G. J. Bagby, R. Siggins II, J. E. Shellito, D. A. Welsh, The lineage–c-Kit$^+$Sca-1$^+$ cell response to *Escherichia coli* bacteremia in Balb/c mice. *Stem Cells* **26**, 1778–1786 (2008).
25. X. Zhao, G. Ren, L. Liang, P. Z. Ai, B. Zheng, J. A. Tischfield, Y. Shi, C. Shao, Brief report: Interferon-γ induces expansion of Lin$^-$Sca-1$^+$C-Kit$^+$ cells. *Stem Cells* **28**, 122–126 (2010).
26. X.-S. He, M. Draghi, K. Mahmood, T. H. Holmes, G. W. Kemble, C. L. Dekker, A. M. Arvin, P. Parham, H. B. Greenberg, T cell–dependent production of IFN-γ by NK cells in response to influenza A virus. *J. Clin. Invest.* **114**, 1812–1819 (2004).
27. J. R. Schoenborn, C. B. Wilson, Regulation of interferon-γ during innate and adaptive immune responses. *Adv. Immunol.* **96**, 41–101 (2007).
28. J. C. Gomez, M. Yamada, J. R. Martin, H. Dang, W. J. Brickey, W. Bergmeier, M. C. Dinauer, C. M. Doerschuk, Mechanisms of interferon-γ production by neutrophils and its function during *Streptococcus pneumoniae* pneumonia. *Am. J. Respir. Cell Mol. Biol.* **52**, 349–364 (2015).
29. R. Yamaguchi, J. Kawata, T. Yamamoto, Y. Ishimaru, A. Sakamoto, T. Ono, S. Narahara, H. Sugiuchi, E. Hirose, Y. Yamaguchi, Mechanism of interferon-gamma production by monocytes stimulated with myeloperoxidase and neutrophil extracellular traps. *Blood Cells Mol. Dis.* **55**, 127–133 (2015).
30. L. Zhang, J. S. Cardinal, P. Pan, B. R. Rosborough, Y. Chang, W. Yan, H. Huang, T. R. Billiar, M. R. Rosengart, A. Tsung, Splenocyte apoptosis and autophagy is mediated by interferon regulatory factor 1 during murine endotoxemia. *Shock* **37**, 511–517 (2012).
31. H. Janols, C. Bergenfelz, R. Allaoui, A. M. Larsson, L. Rydén, S. Björnsson, S. Janciauskiene, M. Wullt, A. Bredberg, K. Leandersson, A high frequency of MDSCs in sepsis patients, with the granulocytic subtype dominating in gram-positive cases. *J. Leukoc. Biol.* **96**, 685–693 (2014).
32. J.-I. Youn, S. Nagarj, M. Collazo, D. I. Gabrilovich, Subsets of myeloid-derived suppressor cells in tumor-bearing mice. *J. Immunol.* **181**, 5791–5802 (2008).
33. J. E. Talmadge, D. I. Gabrilovich, History of myeloid-derived suppressor cells. *Nat. Rev. Cancer* **13**, 739–752 (2013).
34. J. H. DeLong, A. O. Hall, C. Konradt, G. M. Coppock, J. Park, G. Harms Pritchard, C. A. Hunter, Cytokine- and TCR-mediated regulation of T cell expression of Ly6C and Sca-1. *J. Immunol.* **200**, 1761–1770 (2018).
35. M. Otto, *Staphylococcus aureus* toxins. *Curr. Opin. Microbiol.* **17**, 32–37 (2014).
36. Y.-S. Bae, H. Bae, Y. Kim, T. G. Lee, P.-G. Suh, S. H. Ryu, Identification of novel chemoattractant peptides for human leukocytes. *Blood* **97**, 2854–2862 (2001).
37. G. H. Bae, H. Y. Lee, Y. S. Jung, J. W. Shim, S. D. Kim, S.-H. Baek, J. Y. Kwon, J. S. Park, Y.-S. Bae, Identification of novel peptides that stimulate human neutrophils. *Exp. Mol. Med.* **44**, 130–137 (2012).
38. Y.-S. Bae, J. Y. Song, Y. Kim, R. He, R. D. Ye, J.-Y. Kwak, P.-G. Suh, S. H. Ryu, Differential activation of formyl peptide receptor signaling by peptide ligands. *Mol. Pharmacol.* **64**, 841–847 (2003).
39. S. K. Lee, S. D. Kim, M. Kook, H. Y. Lee, J. Ghim, Y. Choi, B. A. Zabel, S. H. Ryu, Y.-S. Bae, Phospholipase D2 drives mortality in sepsis by inhibiting neutrophil extracellular trap formation and down-regulating CXCR2. *J. Exp. Med.* **212**, 1381–1390 (2015).
40. M. Hørder, W. Gerhardt, M. Härkönen, E. Magid, E. Pitkänen, J. H. Strömme, L. Theodorsen, J. Waldenström, Experiences with the Scandinavian recommended methods for determinations of enzymes in blood: A report by the Scandinavian Committee on Enzymes (SCE). *Scand. J. Clin. Lab. Invest.* **41**, 107–116 (1981).

Acknowledgments

Funding: This study was supported by the Basic Science Research Program through the National Research Foundation of Korea (NRF) funded by the Ministry of Science, ICT and Future Planning (NRF-2015R1A2A1A10054567, NRF-2017R1A5A1014560, and NRF-2018R1A2B3003868). **Author contributions:** M.Y.P. designed and performed the research, analyzed the data, and wrote the paper. H.S.K. designed and performed the research, and analyzed the data. H.Y.L. analyzed the data and wrote the paper. B.A.Z. wrote the paper. Y.-S.B. designed the research, analyzed the data, and wrote the paper. **Competing interests:** The authors declare that they have no competing interests. **Data and materials availability:** All data needed to evaluate the conclusions in the paper are present in the paper and/or the Supplementary Materials. Additional data related to this paper may be requested from the authors.

Submitted 2 May 2019
Accepted 21 November 2019
Published 22 January 2020
10.1126/sciadv.aax8820

Citation: M. Y. Park, H. S. Kim, H. Y. Lee, B. A. Zabel, Y.-S. Bae, Novel CD11b$^+$Gr-1$^+$Sca-1$^+$ myeloid cells drive mortality in bacterial infection. *Sci. Adv.* **6**, eaax8820 (2020).